Geoderma 163 (2011) 265–274

Contents lists available at ScienceDirect

Geoderma

journal homepage: www.elsevier.com/locate/geoderma

Revisiting ferrolysis processes in the formation of Planosols for rationalizing the soils with stagnic properties in WRB

E. Van Ranst [a,*], M. Dumon [a], A.R. Tolossa [a,b], J.-T. Cornelis [c], G. Stoops [a], R.E. Vandenberghe [d], J. Deckers [e]

[a] Department of Geology and Soil Science (WE13), Ghent University, Krijgslaan 281/S8, B-9000 Gent, Belgium
[b] Department of Natural Resources Management, Jimma University College of Agriculture and Veterinary Medicine, Ethiopia
[c] Earth and Life Institute (Environmental Sciences), Université Catholique de Louvain, Croix du Sud 2/10, B-1348 Louvain-la-Neuve, Belgium
[d] Department of Physics and Astronomy, Ghent University, Proeftuinstraat 86, 9000 Gent, Belgium
[e] Department of Earth and Environmental Sciences, Catholic University of Leuven, Celestijnenlaan 200E, B-3001 Heverlee, Belgium

ARTICLE INFO

Article history:
Received 4 January 2011
Received in revised form 8 April 2011
Accepted 1 May 2011
Available online 23 May 2011

Keywords:
Planosols
Ferrolysis
Stagnic properties
Stagnosols
WRB

ABSTRACT

Planosols have been recognized as a Major Soil Group right from the beginning in the legend of the FAO/Unesco Soil Map of the World. Also in WRB system it maintained that position at Reference Soil Group level on the account that a major pedogenetic process, ferrolysis, is underlaying the severe stagnic properties that characterize this group. With the introduction of Stagnosols in WRB in 2006, it appears that a serious overlap has been introduced at Reference Soil Group level. This paper aims to throw new light on the genesis of Planosols, drawing from new soil surveys conducted in the south-western Ethiopian highlands. Representative soil profiles were sampled and analyzed for their physico-chemical, mineralogical and micromorphological properties, and a hypothesis has been forwarded to explain the formation of these Planosols. The conclusion is that it is highly unlikely that 'ferrolysis' can be called upon to explain the genesis of Planosols in the Ethiopian highlands, and an alternative geogene hypothesis is put forward to explain the formation of these duplex soils. As Ethiopia is one of the mainstays of Planosols, it is suggested that WRB rethinks its strategy on soils with stagnic properties as there is room for rationalization in view of a generally felt overlap between Planosols and Stagnosols. WRB could rationalize by sub-dueing either the Planosols or the Stagnosols to a lower level.

1. Introduction

The Reference Soil Group of Planosols holds soils with surface horizons that are bleached and light-colored or have a stagnic color pattern, show signs of periodic water stagnation and abruptly overly a dense, slowly permeable subsoil with significantly more clay than the surface horizons (Driessen et al., 2001; IUSS Working Group WRB, 2007). They typically occur in seasonally or periodically wet plateau areas, often above normal flood levels or nearby rivers or estuaries. Occasionally they occur on gentle or very gentle slopes, but usually the geographical extent is limited in these landscape positions.

In the old European literature, these soils are mainly referred to as pseudogley soils or as clayey Podzols, however, neither of these soil groupings required an abrupt textural change from the bleached horizon to the underlying dense horizon (Dudal, 1971). The U.S. classification of 1938 (Baldwin et al., 1938) was the first to use the term Planosols; the present Soil Taxonomy (Soil Survey Staff, 2010) includes most of the original Planosols in the Albaqualfs, Albaquults and Argialbolls. Planosols are occurring as major soil unit in the Legend of the FAO-Unesco Soil Map of the World (FAO-Unesco, 1974). In the revised legend of the Soil Map of the World (FAO-Unesco, 1990), Planosols are recognized as a major soil grouping at highest level and so they were in the first ISSS-endorsed version of WRB (FAO/ISRIC/ISSS, 1998). Also in the World Reference Base for Soil Resources (IUSS Working Group WRB, 2007), Planosols are accommodated under the set of soils with stagnating water together with the Stagnosols.

The WRB (IUSS Working Group WRB, 2007) accommodates four Reference Soil Groups at the highest level, which have an assemblage of soil features indicative for water stagnation within the soil profile: in key order they are the Solonetz, the Planosols, the Stagnosols and the Albeluvisols. It is acknowledged that water stagnation is not part of the key definition in Solonetz and in Albeluvisols, however in most cases it is a major feature in these soils. Stagnosols had a turbulent history in the WRB. In the first draft of WRB in 1994 (FAO/ISRIC/ISSS, 1994) they were proposed as a reference group, however they did not make it in the 1998 version (FAO/ISRIC/ISSS, 1998). The Working Group WRB at that time did recognize the importance of water stagnation as an important soil feature. The rationale for not keeping the Stagnosols in was the fact that water stagnation as such is only a consequence rather than a major pedogenetic process. This was in conflict with one of the basic principles of WRB to follow as much as possible a soil-genetic approach in the delineation of major soil groupings.

* Corresponding author. Tel.: +32 (0)9 264 46 26; fax: +32 (0)9 264 49 97.
E-mail address: eric.vanranst@ugent.be (E. Van Ranst).

0016-7061/$ – see front matter © 2011 Elsevier B.V. All rights reserved.
doi:10.1016/j.geoderma.2011.05.002

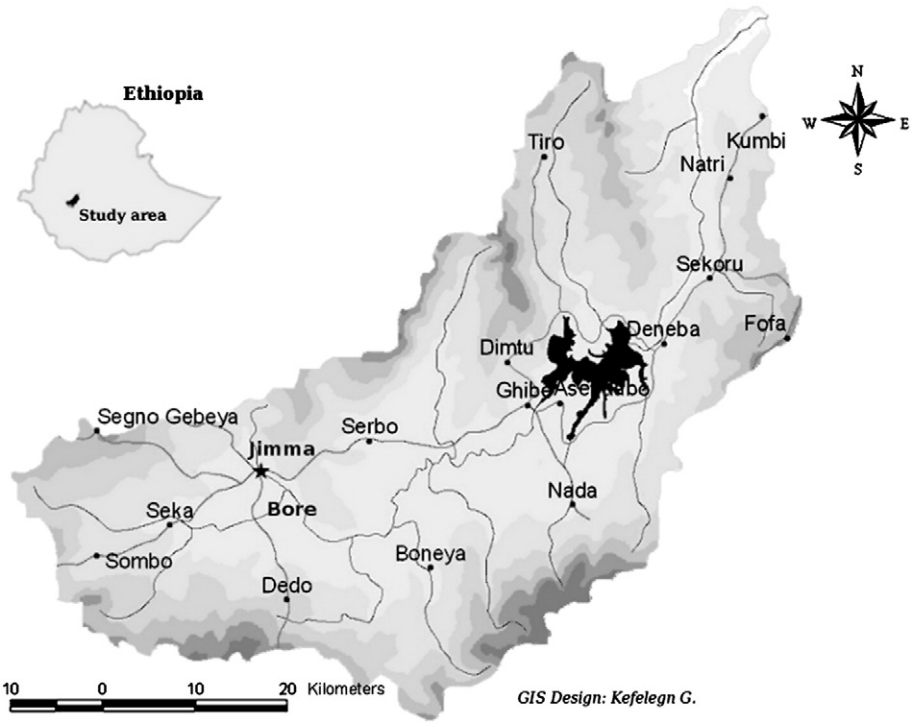

Fig. 1. Location of the Gilgel Gibe catchment and the Bore valley where the profile discussed in detail in this paper is located.

In line with the above-sketched rationale, the following pedogenetic processes were considered important for recognizing the soils with stagnic properties: (1) *Solonetz*: sodification, peptisation of the clay minerals which move into a very compact argic horizon. Upon solodisation of the Solonetz, it is hypothesized that the distinct textural change and the water stagnation is enhanced by a ferrolysis process at the fringe between the E and the B horizon hence the whitish silt-capping on top of the columns of the natric horizon; (2) *Planosols*: the 'abrupt textural change' from the coarse textured surface soil to the finer subsoil can be a result of (a) 'geogenetic processes' such as sedimentation of sandy over clayey layers, creep or sheet wash of lighter textured soil over clayey material, colluvial deposition of sandy over clayey material, or selective erosion whereby the finest fraction is removed from the surface layers, and/or (b) 'physical pedogenetic processes', such as selective eluviation–illuviation of clay in soil material with a low structural stability, and/or (c) 'chemical pedogenetic processes' notably a process proposed under the name 'ferrolysis', an oxidation–reduction sequence driven by chemical energy derived from bacterial decomposition of soil organic matter (Brinkman, 1970); and (3) *Albeluvisols*: the genesis of Albeluvisols roots back to Late Glacial times, more particularly to the Middle and the Younger Dryas periods and its respective interstadials: argilluviation (mobilization and translocation of clay) during interglacials and formation of polygonal albeluvic tonguing during the last glacial period, including compaction of the outer sphere of the soil polygons leading to the so-called 'closed box system' which eventually results in strongly expressed water stagnation on top of the compacted argic horizon. It was also inferred that the process of ferrolysis could have enhanced the textural contrast in Albeluvisols, however this claim was refuted by Van Ranst and De Coninck (2002), who proved that this process does not take place in soils with albeluvic tonguing (Albeluvisols) and in soils with stagnic color pattern in Western Europe.

During the international conference on soil classification in 2004, at Petrozavodsk (Russian Federation, organized by the Institute of Biology, Karelian Research Centre), the decision was taken to take the Stagnosols on board again in WRB. This decision was implemented in the published 2006 and 2007 (electronic) versions of WRB during the IUSS congress at Philadelphia, USA. At the same time a call was made for fundamental research which should elucidate the above-mentioned pedogenetic processes and especially the process of ferrolysis.

Fig. 2. A typical Vertic Planosol of the Gilgel Gibe catchment showing sub-soil gilgai and nicely developed slickensides (see inset) in the subsoil.

Table 1
Color and texture of the soil layers sampled in the Bore profile at 5 cm intervals.

Horizon	Depth (cm)	Color (dry)	Clay		Silt		Sand	
			<2 μm		2–63 μm		63 μm–2 mm	
			SS[a]	PM[b]	SS[a]	PM[b]	SS[a]	PM[b]
Ap/E	5–10	10YR 7/1	27	26	69	69	4	5
E	10–15	10YR 7/1.5	27	24	69	72	4	4
E	15–20	10YR 7/2	26	26	70	71	4	4
E	20–25	10YR 7/2	24	25	72	71	4	4
E	25–30	10YR 7/2.5	23	25	73	71	4	3
E	30–35	10YR 7/2	23	25	73	71	4	3
Ecg	35–40	10YR 7/1.5	25	26	67	66	8	8
Bw	40–45	10YR 4/1	63	69	30	25	7	6
Bw	45–50	10YR 3/1	70	74	25	21	5	5
Bw	50–55	10YR 3/1	69	73	26	23	5	4
Bw	70–75	10YR 3/1	70	74	25	22	5	5

[a] Successive sedimentation method.
[b] Pipette method of Köhn.

The soil-forming process, termed ferrolysis, was proposed by Brinkman (1970), to explain clay decomposition and interlayering in acid, seasonally wet soils. Ferrolysis involves cyclic reduction and oxidation of iron in an open system that allows evacuation of the reduced solution from the ferrolysed area (Barbiero et al., 2010). During the reduction phase, iron (III) oxides are reduced and the ferrous iron formed displaces exchangeable cations, including Al, on the silicates with surface charge. During the oxidation phase, ferrous iron is oxidized to ferric hydroxide and hydrogen ions. The acidic environment is conducive to clay mineral decomposition. The hydrogen ions displace the exchangeable ferrous iron and release lattice cations from the clay minerals. In every cycle, soluble cations and part of Al, as soluble polymers, are leached; part of the clay mineral lattice is destroyed, and the profile texture becomes more differentiated. Since the introduction by Brinkman, ferrolysis has been extensively reported in literature in the 1970s and 1980s as the process partly or completely responsible for textural contrast of soils where bleaching and mottling are predominant morphological features (e.g. Brinkman et al., 1973; Chartres, 1987; Dijkerman and Miedema, 1988; Feijtel et al., 1988). More recent studies suggest ferrolysis as a "probable" (often without well-founded arguments) process to explain Fe–Mn-oxides segregations, gleying, chloritization (Singh et al., 1998), textural variation and low pH in soils (Boixadera et al., 2003; O'Geen et al., 2008; Schaefer et al., 2002). Since the eighties, several studies also have questioned the incidence of ferrolysis and indicated that ferrolysis as process to destroy open 2:1 clay minerals and to form soils with contrasting texture has been overestimated (Boivin et al., 2004; Eaqub and Blume, 1982; Favre et al., 2002; Montagne et al., 2008; Van Ranst and De Coninck, 2002). Meanwhile, few studies are based on the monitoring of the physico-chemical characteristics of the soil solutions to validate or not the occurrence of ferrolysis as the transformation process (Barbiero et al., 2010; Boivin et al., 2002; Hobson and Dahlgren, 1998).

As Planosols are most extensive in relatively hot climates with a strong seasonal variation in rainfall, they are commonly occurring in association with Vertisols in presently sub-humid to semi-arid climates. In these zones, all variations of intermediates between Vertisols and Planosols occur such as Vertisols with a thin layer of gray or light gray, silty upper soil horizon of variable thickness, overlaying heavy clay, with sometimes silty material etched in along cracks into the underlying clayey material. If this layer of silty material is only few centimetres thick, the Vertisol still stands and this coarse material is tell-tale of some important pedogenetic process which is not sufficiently understood.

Soilscapes with associations of Planosols and Vertisols are very common throughout the Ethiopian highlands, all developed from massive occurrences of Tertiary flood basalts under a sub-humid moisture regime. In the framework of a major research project in Gilgel Gibe catchment in the Omo-River basin, Vertic Planosols were sampled and studied to throw new light on the genesis of these soils, so as (1) to contribute to the scientific debate on the origin of the abrupt textural change in Planosols and (2) to provide scientific ground to the IUSS Working Group WRB for rationalizing the Key to the Reference Groups.

2. Materials and methods

2.1. Environmental setting

The Gilgel Gibe catchment, covering an area of 5500 km^2, is located in south-western Ethiopia, in the Oromiya region, about 260 km of Addis Ababa (Fig. 1). The Gilgel Gibe, the main river of the catchment, is a tributary of the Gibe river which on its turn is a tributary of the Omo River. The geology of the catchment is very complex and is dominated by Eocene and Paleocene volcanic rocks, related to the East African rift valley (Tadesse et al., 2003). Many remnant volcanic landforms, such as cone structures, lava flows, mudflows, plugs, etc. can readily be recognized in the landscape. The volcanic rocks and materials identified in the field include basalts (hawaiites), trachytes, rhyolites, tuffs, ignimbrites and ash deposits. The altitude in the catchment varies between 1096 and 3259 m.a.s.l. The lower valley areas along the river are filled up with alluvium and lacustrine sediments. The climate of the Gilgel Gibe area is sub-humid. The main rains fall between May and September. The mean annual rainfall in the catchment increases from 1300 mm in the lower valley areas to 2000 mm in the highest regions. Temperature is fairly constant throughout the year, with the mean minimum, maximum and average temperatures at 1800 m altitude (Jimma station) being 11 °C, 25 °C and 17 °C, respectively. The major reference soil groups in the catchment are Nitisols, Acrisols, Ferralsols, Vertisols and Planosols. The soilscapes, with associations of Planosols and Vertisols, are mainly used for grazing.

Table 2
Chemical characteristics of the fine earth fraction of soil layers sampled in the Bore profile at 5 cm intervals.

Horizon	Depth (cm)	pH H_2O	pH KCl	OC (%)	N (mg/kg)	C/N	Exchange complex ($cmol_c\ kg^{-1}$)					BS (%)
							CEC	Ca	Mg	K	Na	
Ap/E	5–10	5.2	4.1	3.1	2642	12	20.7	6.0	1.2	0.7	0.2	38
E	10–15	5.3	4.0	1.8	1675	11	16.1	5.0	0.9	0.2	0.2	40
E	15–20	5.2	4.0	0.9	998	9	13.0	4.0	0.9	0.1	0.2	38
E	20–25	5.1	4.0	0.7	599	12	10.0	3.3	0.7	0.1	0.2	43
E	25–30	5.3	4.1	0.5	408	12	8.8	3.4	0.7	0.1	0.2	51
E	30–35	5.6	4.1	0.4	284	14	8.8	4.3	0.8	0.1	0.3	62
Ecg	35–40	5.6	4.2	0.4	353	11	11.0	5.4	1.2	0.1	0.3	64
Bw	40–45	5.9	4.2	1.1	878	13	45.9	26.2	6.4	0.7	0.7	74
Bw	45–50	6.0	4.2	0.9	801	11	52.0	32.7	7.9	0.7	0.8	81
Bw	50–55	5.8	4.4	0.9	633	14	51.9	33.8	7.6	0.8	0.8	83
Bw	70–75	6.0	4.6	0.8	669	12	53.1	35.9	9.0	0.8	0.8	87

2.2. Materials

Planosols occurring in the flat, lower river terraces of the Gilgel Gibe catchment (Fig. 1) in the south-western Ethiopian highlands were surveyed during a long lasting terrain study using aerial photographs followed by weeks of soil transect studies by auger observations. The position of soil observations was recorded using a GPS (UTM 37°N coordinates) and the description of soil profiles was made according to the FAO field guidelines (FAO, 2006). The typical Planosols in this catchment have an abrupt textural change at about a depth of 40 cm separating a bleached, silty topsoil from a heavy clayey Stagnic Vertisol (Manganiferric, Pellic). This buried Vertisol clearly shows surface as well as sub-soil gilgai and has nicely developed intersecting slickensides in the subsoil (Fig. 2). A representative soil profile in the Bore valley (Fig. 1) at 1,716 m .a.s.l. was selected for more detailed analysis. The Vertic Planosols in the Bore valley have, under a well rooted Ap horizon of 8–10 cm thick, a bleached, (dark) gray (10YR 4–5/1, moist) to light gray (10YR 7/2, dry), silty E(g) horizon with crumby structure and diffuse mottling, that abruptly overlays a black (10YR 2–3/1, moist and dry), heavy clayey vertic horizon with sometimes silty material etched in along cracks into the vertic material. Many sharp, black, nodular concretions occur at the abrupt textural change. A transect augered in the Bore valley, from the hillside towards the alluvial valley, showed that the thickness of the bleached horizon slightly decreases in the direction of the river. The local name 'Bore' means 'white', referring to the color of the bleached layer, which at this site and also at other sites in the catchment, is used by the local communities for brick-making. Bulk samples of a representative Bore soil profile were taken at fixed depth intervals (of every 5 cm down into the vertic material up to 75 cm below the soil surface) for physico-chemical and mineralogical analyses, whereas undisturbed and oriented samples were taken using Kubiëna boxes for the preparation of thin sections. Bulk samples were homogenized and reduced in volume using a Rifle Jones sample splitter, followed by air-drying, light pulverization, and dry sieving using a 2 mm sieve.

2.3. Laboratory procedures

Most analyses were performed on air-dry fine earth (<2 mm) according to the procedures described in Van Ranst et al. (1999). Soil textural analysis was done using pipette method after removal of organic matter with H_2O_2 and by quantitative recovery of clay, silt and sand fractions after sieving and successive sedimentation. From the fine-earth fraction, the sand (2000–63 μm) fraction was separated by sieving, and the clay (<2 μm) was separated from the silt (63–2 μm) by successive sedimentation. During clay separation, Na_2CO_3 was used as dispergent and NaCl as flocculation agent. The recovered clay was thoroughly washed with alcohol to remove excess Cl^- (till testing negative with $AgNO_3$), centrifuging at about 3500 rpm after each step. Separated fractions were used for mineralogical analysis. The soil pH was measured potentiometrically in a 1:2.5 (W/V) suspension of H_2O and 1 *M* KCl. Organic carbon determination followed the Walkley–Black wet combustion method. Cation exchange capacity (CEC) and exchangeable base cations (Ca, Mg, K, and Na) were determined by leaching with 1 *M* ammonium acetate (pH 7) using a Centurion mechanical vacuum extractor. The exchangeable base cations in the leachate were measured by atomic absorption spectroscopy (AAS).

The total elemental composition of each sample was determined after: (1) fusion with Li_2CO_3 and H_3BO_3 at 1000 °C and dissolution in HCl for determination of Si and Al with AAS in a N_2O flame; and (2) a

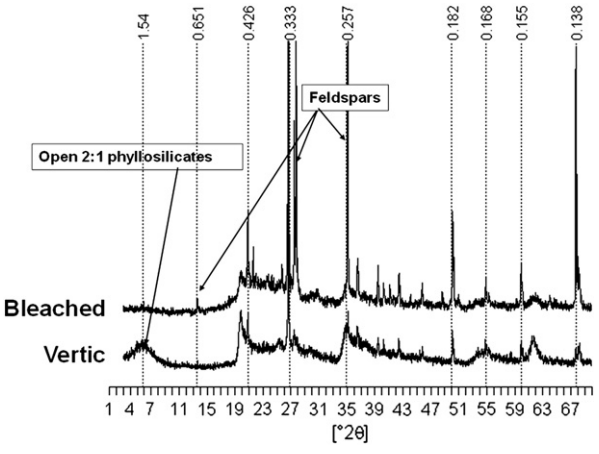

Fig. 3. XRD patterns of non-oriented powder samples of total soil of the bleached and the vertic horizon. Units are expressed in nanometers.

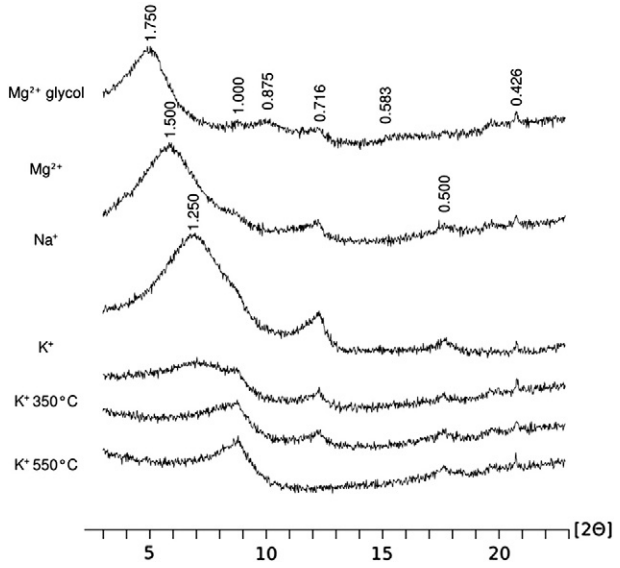

Fig. 4. XRD patterns of the treated clay fraction of the vertic horizon. Units are expressed in nanometers.

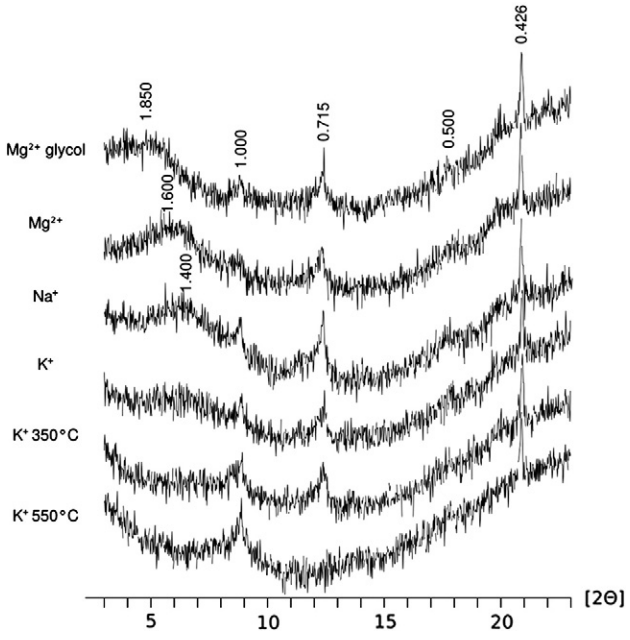

Fig. 5. XRD patterns of the treated clay fraction of the bleached horizon. Units are expressed in nanometers.

Table 3
Total elemental composition of the fine earth of soil layers sampled in the Bore profile at 5 cm depth intervals.

Contents	Depth (cm)										
	5–10	10–15	15–20	20–25	25–30	30–35	35–40	40–45	45–50	50–55	70–75
SiO_2	72.14	75.77	78.05	77.37	78.52	79.4	76.53	53.56	54.03	54.07	55.08
Al_2O_3	5.02	4.96	4.53	5.59	5.08	5.22	4.99	11.06	13.65	14.04	13.28
Fe_2O_3	3.96	3.46	3.63	3.64	3.68	4.07	7.02	14.4	10.35	10.19	9.54
TiO_2	1.32	1.44	1.56	1.66	1.72	1.6	1.55	1.02	1.06	0.99	1.03
MnO	0.09	0.06	0.06	0.05	0.05	0.05	0.27	0.31	0.31	0.31	0.37
CaO	0.21	0.18	0.15	0.15	0.1	0.17	0.17	0.74	0.93	0.82	1.1
MgO	0.19	0.13	0.15	0.15	0.15	0.14	0.09	0.27	0.3	0.35	0.39
Na_2O	1.22	1.06	1.17	1.24	1.21	1.28	1.18	0.45	0.45	0.43	0.53
K_2O	3.3	3.03	3.29	3.55	3.68	2.14	1.83	1.12	1.21	1.27	1.43
P_2O_5	0.06	0.04	0.03	0.02	0.02	0.02	0.02	0.04	0.03	0.03	0.02
H_2O-	2.57	2.36	1.93	1.52	1.39	1.37	1.7	6.96	7.81	7.91	8.2
H_2O+	9.32	6.74	5.28	4.28	3.64	3.58	4.25	9.58	9.41	9.05	8.65
Total	99.4	99.22	99.81	99.2	99.23	99.03	99.61	99.51	99.54	99.45	99.63

treatment with $HF + HNO_3 + HClO_4$ and dissolution of the evaporation residue in HCl, for determination of Fe, Ca, Mg, K, Na and Mn (AAS in an air-acetylene flame) and for determination of Ti and P (colorimetry) (Ingamells, 1966; Omang, 1969). Loss on ignition (H_2O^-, H_2O^+) was determined by heating the samples at 105 and 1000 °C, respectively.

X-ray diffraction (XRD) analysis was performed on non-oriented powder bulk samples and on clay samples oriented on glass slides, the latter involving standard treatments (Mg saturation followed by glycolation, K saturation followed by heating at 350 °C and 550 °C) (Whittig and Allardice, 1986). All XRD patterns were collected with a Philips X'pert System (Cu-Kα radiation, scan time 1 s per 0.02° 2-theta).

Thin sections, mostly 9 by 6 cm large, were prepared of oriented samples, after impregnation with a cold-setting polyester resin, added before applying vacuum conditions (Benyarku and Stoops, 2005). Descriptions were made using the concepts and terms proposed by Stoops (2003).

Mössbauer spectra (MS) were collected at room temperature (RT) and at 80 K for the Fe nodules. A spectrometer operating in constant acceleration mode with triangular reference signal and a ^{57}Co (Rh) source were used. Accumulation of the data was performed in 1024 channels using the WISSEL CMCA-550 unit and continued until a background of 10^6 counts was reached. The spectrometer was calibrated by collecting the spectrum of a standard α-Fe_2O_3 powder at RT. The MS were computer analyzed in terms of model-independent distributions of hyperfine-parameter values (Vandenberghe et al., 1994).

Dark oxalate (o) extractable Si, Al and Fe and dithionite–citrate–bicarbonate (DCB) (d) extractable Fe, Al, Si and Mn were determined according to Dahlgren (1994) and using AAS for quantification.

3. Results and discussion

3.1. Evidence for lack of ferrolysis processes

The two methods used for textural analysis give similar results (Table 1) and show that both, bleached (10YR 7/2, dry) and black (10YR 3/1, dry), vertic, soil materials are very homogeneous in their granulometric composition. Both horizons have a very similar low sand content (5%), but show marked difference in their clay and silt content. The bleached, silty (69–73% silt) E horizon abruptly overlays the heavy clayey (63–74% clay) Bw horizon; an increase in clay content of about 40% at around 40 cm depth. If 2:1 clay minerals, representing a 40% decrease in clay content in the bleached layer, would have been destroyed by ferrolysis, not only the silt content but also the sand content should show an remarkable increase in the bleached layer.

The transition between the two soil materials is, besides an abrupt change in texture, also indicated by significant changes in chemical characteristics (Table 2). At the transition (depth around 40 cm), the OC content increased from 0.4 to 1.1% suggesting a buried topsoil or migration of organic matter. Also an increase in N content is noticed in the vertic horizon. The strong increase in CEC, from 9–10 in the lower E horizons to 46–53 cmol(+)/kg in the vertic or Bw horizons, and also in exchangeable base cations (Table 2) clearly reflects differences in mineralogical composition. Along the same line are the calculated CEC-clay values (not given) which jump from 38 cmol(+)/kg in the E-horizon to 75 cmol(+)/kg in the Bw horizon. Soil pH (in H_2O) and base saturation gradually increase with soil depth, but are higher than 5.1 and 38% in all horizons, respectively. The relatively high pH

Table 4
Principal micromorphological characteristics of the bleached and vertic horizons.

Horizon	Bleached (E) horizons	Vertic (Bw) horizons
Microstructure	Blocky and fine blocky with granular aspect, sometimes grading to vughy and spongy; channels	Angular accommodating blocky (1 mm) with some channels
Groundmass		
Coarse material	Dominantly fine sand and silt sized opal phytoliths, some quartz grains, some colourless volcanic glass fragments; few medium sand sized angular grains of feldspar and quartz	Dominantly fine sand and silt sized opal phytoliths some quartz grains; few medium sand sized angular grains of feldspar and quartz
Micromass	Grayish, strongly speckled; undifferentiated b-fabric	Yellowish gray, weakly speckled; clear parallel-poro-granostriated b-fabric
C/f 10 μm related distribution	Close porphyric	Open porphyric
Pedofeatures		
	Irregular, diffuse, moderately impregnated brownish iron oxide nodules	Rounded, sharp, strongly impregnated dark brown to opaque iron/manganese oxide nodules, often with concentric fabric
	Infillings with Bw material	Infillings with E material, often stress deformed
	Granular channel infillings	Fragments of limpid, yellowish clay coatings with strong continuous orientation, often stress deformed, then with striated orientation or kink-band fabric

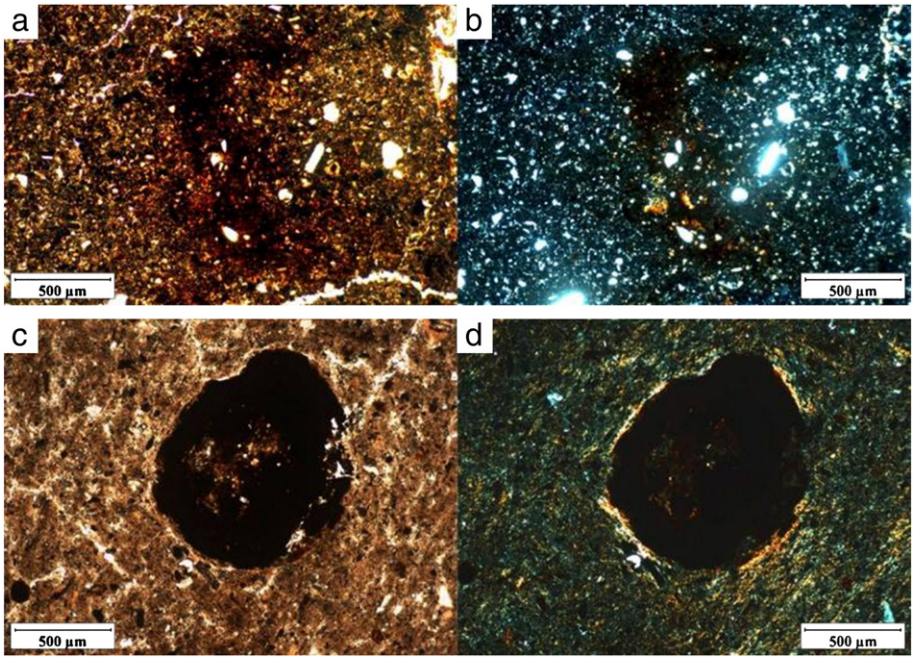

Fig. 6. Diffuse iron nodules in the groundmass of the bleached horizon in plane (a) and crossed (b) polarized light and disorthic iron nodules in the groundmass of the vertic horizon in plane (c) and crossed (d) polarized light.

(5.6) and base saturation (above 60%) at present just above the textural break indicate that the present conditions are not inductive for ferrolysis. X-ray diffraction diagrams of non-oriented powder bulk samples (Fig. 3) shows that (i) quartz (0.426, 0.333, 0.182, 0.168, 0.155 and 0.138 nm) and feldspars (0.651, 0.322 and 0.257 nm) are the major crystalline mineral components in the upper bleached soil horizon, while these minerals are present in much lower contents in the vertic horizon. The XRD diagram of the latter horizon shows a clear broad reflection at 1.54 nm indicative for open 2/1 phyllosilicates. The XRD diagrams of the clay fraction of the vertic horizon after standard treatments are displayed in Fig. 4. These diagrams show that the clay fraction is dominated by smectites (1.25 nm Na^{+}-saturated; 1.50 nm Mg^{2+}-saturated; 1.75 nm after glycolation and gradually collapsing to 1.00 nm after K^{+}-saturation and heating). Minor amounts of illite (1.00 nm), kaolinite (0.716 nm) and quartz (0.426 nm) seem to be present as well. The XRD diagrams of the clay fraction of the bleached horizon (Fig. 5) show a dominance of kaolinite (reflection at 0.715 nm disappearing after heating at 550 °C), illite (1.00 and 0.500 nm), quartz (0.426 nm) and some minor indications of smectitic minerals. The diffused broad diffraction band centered at about 0.4 nm (not shown) indicates opal-A or phytoliths (Drees et al., 1989). The upper soil horizon (Table 3) has much higher total SiO_2 (72.1–79.4%), Na_2O (1.1–1.3%) and K_2O (1.8–3.7%) contents compared to the clayey subsoil (53.6–55.1% SiO_2, 0.4–0.5% Na_2O and 1.1–1.4% K_2O), indicating the dominance of siliceous components, feldspars and volcanic glass in the upper horizon. The presence of these mineral components is in contradiction with a weathering by ferrolysis. Also the increase of Ti in the E layers seems insufficient to explain the genesis by destruction of the weatherable minerals by ferrolysis. At the transition (40 cm depth), there is a clear increase in the Al_2O_3, CaO, MgO, and H_2O (loss on ignition) content, due

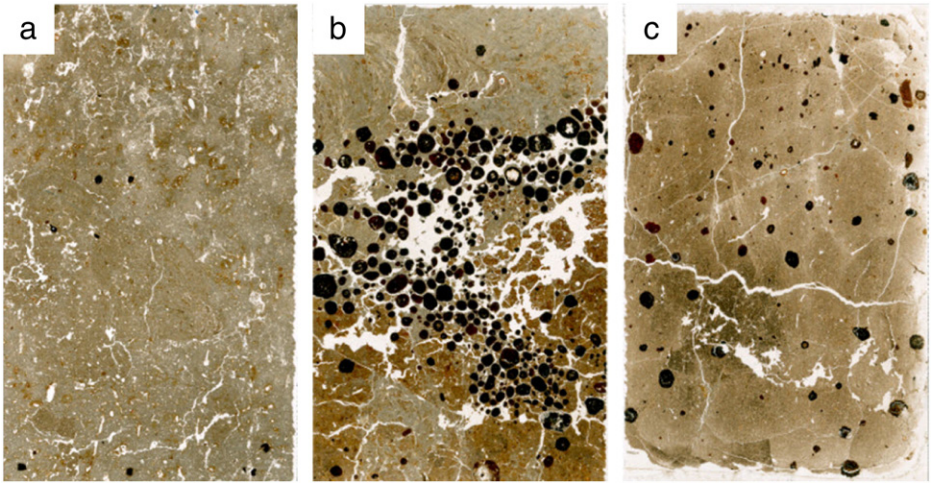

Fig. 7. Scanned thin sections (60 mm × 90 mm) showing the distribution of disorthic iron nodules in the Planosols: (a) almost completely absent in the bleached horizon; (b) high concentration at the abrupt textural change; and (c) a low amount in the vertic horizon.

Table 5
Total Fe_2O_3, MnO and P_2O_5 contents (in wt.%) in the nodules present on top and in the vertic horizon.

	Fe_2O_3	MnO	P_2O_5
Top vertic	38.20	5.97	0.05
Vertic	39.51	7.30	0.03

to the smectitic minerals, dominating the clay fraction of the vertic horizon, while kaolinite and opal-A dominate the clay fraction in the bleached horizon.

The principal micromorphological characteristics are summarized in Table 4. Important is the presence of many phytoliths and some volcanic glass fragments in the coarse fraction of the bleached horizons. Especially the open porphyric c/f related distribution pattern of the Bw horizons, with the strongly expressed striated b-fabric, the disorthic, nearly opaque nodules and the stress deformed clay coatings (striated orientation, locally kink-band fabric) correspond to a typical vertic material as described by Kovda and Mermut (2010). An important pedofeature of these soils are the iron oxide nodules; diffuse and moderately impregnated nodules (Fig. 6a and b) in the bleached horizon, and sharp, strongly impregnated, mainly concentric iron/manganese nodules (Fig. 6c and d) in the vertic horizon. The latter are directly surrounded by a grano-striated b-fabric resulting from the swelling–shrinking processes. Fig. 7 shows the distribution of the disorthic iron nodules in scanned half mammoth thin sections representing the bleached (Fig. 7a), the abrupt transition between E and Bw horizons (Fig. 7b) and the vertic horizon (Fig. 7c). The nodules

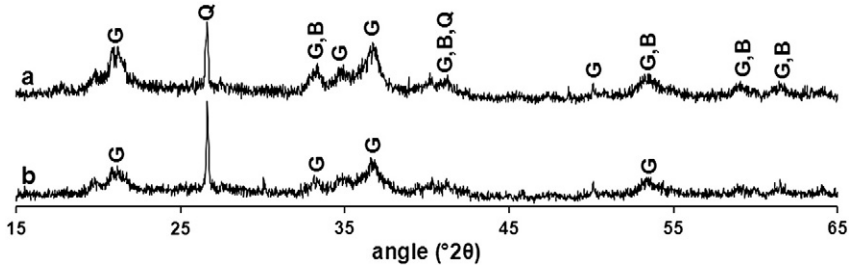

Fig. 8. XRD patterns of grinded iron nodules accumulated at the abrupt textural change and in the vertic horizon (G: goethite; B: bixbyite; Q: quartz).

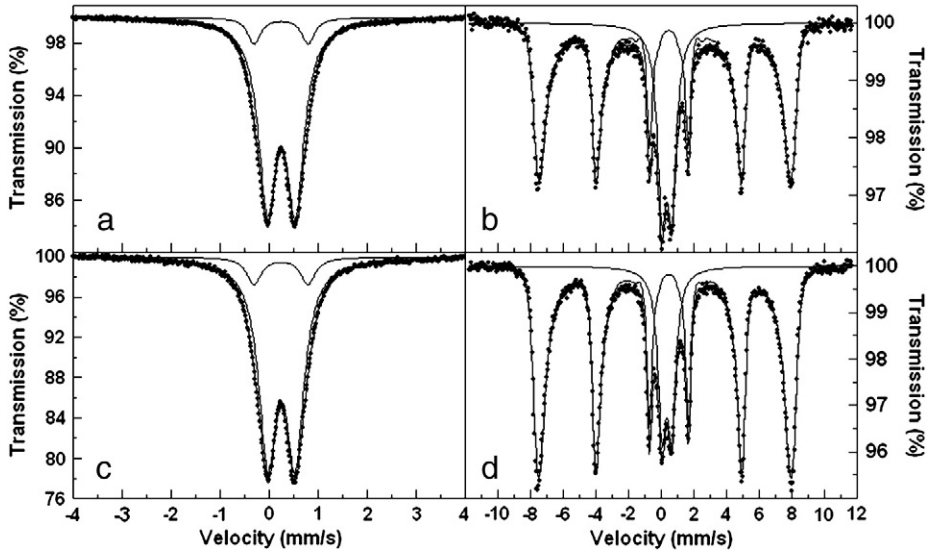

Fig. 9. Mössbauer spectra of the disorthic iron nodules accumulated at the abrupt textural change at room temperature (a) and at 80 K (b), and of those present in the vertic horizon at RT (c) and at 80 K (d).

Table 6
Hyperfine parameters of the spectra of the nodules below and just above the textural break in the Bore profile.

Sample	T (K)	$H_{hf,p}$ (T)	$H_{hf,a}$ (T)	$2\varepsilon_Q$ (mm/s)	δ_{Fe} (mm/s)	ΔE_Q (mm/s)	RA (%)	Assignment
Accumulated nodules	RT	–	–	–	0.36	0.57	90	Goethite (D) + Bixbyite (8a) + other Fe^{3+} compound(s)
		–	–	–	0.37	1.1	10	Bixbyite (24 d)
	80	47.8	43.8	−0.24	0.47	–	72	Goethite (S)
		–	–	–	0.47	0.62	28	Goethite (D) + Bixbyite + other Fe^{3+} compound(s)
Nodules in vertic horizon	RT	–	–	–	0.37	0.56	90	Goethite (D) + Bixbyite (8a) + other Fe^{3+} compound(s)
		–	–	–	0.36	1.1	10	Bixbyite (24 d)
	80	48.0	44.9	−0.24	0.47	–	80	Goethite (S)
		–	–	–	0.47	0.60	20	Goethite (D) + Bixbyite + other Fe^{3+} compound(s)

$H_{hf,p}$ = most probable hyperfine field; $H_{hf,a}$ = average hyperfine field; $2\varepsilon_Q$ = quadrupole shift (sextet); δ_{Fe} = isomer shift refered to metallic Fe; ΔE_Q = quadrupole splitting (doublet); RA = relative area.

Table 7
Si, Al and Fe contents extracted with oxalate and Si, Al, Fe and Mn contents extracted with DCB in soil layers sampled in the Bore profile at 5 cm intervals.

Horizon	Depth (cm)	Oxalate extractable (%)			DCB extractable (%)			
		Si	Al	Fe	Si	Al	Fe	Mn
Ap/E	5–10	0.02	0.08	0.46	1.21	0.26	0.83	0.04
E	10–15	0.05	0.10	0.35	1.57	0.39	0.80	0.01
E	15–20	<0.01	0.06	0.29	1.54	0.31	0.81	0.00
E	20–25	<0.01	0.05	0.28	0.82	0.24	0.86	0.01
E	25–30	<0.01	0.04	0.26	0.66	0.30	1.12	0.00
E	30–35	<0.01	0.03	0.24	1.23	0.39	1.54	0.01
Ecg	35–40	<0.01	0.04	0.42	0.88	0.26	2.94	0.03
Bw	40–45	0.06	0.16	0.50	1.13	0.39	5.12	0.64
Bw	45–50	0.04	0.18	0.44	0.57	0.31	3.27	1.84
Bw	50–55	0.06	0.18	0.39	0.78	0.31	2.63	0.33
Bw	70–75	0.08	0.16	0.31	1.71	0.21	2.12	0.76

are almost completely absent in the bleached horizon. At the abrupt transition between the E and the Bw material (Fig. 7b) the rounded, sharp opaque nodules are strongly concentrated, sometimes packed without interstitial material. In that case they are surrounded by a coating of Bw material, which in turn is covered by a coating of E material. A much lower amount of disorthic nodules is present in the vertic horizon (Fig. 7c).

Chemical analysis (Table 5), combined with XRD (Fig. 8) and Mössbauer spectroscopy (Fig. 9) of the sharp nodules present at the abrupt textural change and in the vertic horizon shows that they have a similar composition: goethite, Fe–Mn oxides and quartz indicated by the sharp reflections. Moreover, the hyperfine parameters (Table 6) indicate that goethite has a comparable degree of crystallinity in both samples (Vandenberghe et al., 1990; 2000). The doublet at RT for both samples (Fig. 9a and c) has firstly been fitted with a quadrupole distribution which yields, in addition to a quadrupole splitting around 0.6 mm/s, a peak at about 1.1 mm/s. The latter can be attributed to the $FeMnO_3$ (bixbyite) doublet originated from the 24 d sites (Banks et al., 1966). The MS spectra at RT were therefore further analyzed with two doublets. The doublet that remains at 80 K (Fig. 9b and d) can also to some extent be assigned to $FeMnO_3$. Because the 8a sites from bixbyite are expected to give a doublet with low quadrupole splitting (~0.66 mm/s) and with half of the intensity of the 24 d doublet (Banks et al., 1966), the remaining part of the doublet must be assigned to very poorly crystallized goethite or to other Fe^{3+} compounds. All these results suggest that all sharp nodules were originally formed in the vertic horizon.

The oxalate and DCB extractable amounts of Si, Al and Fe are given in Table 7. The oxalate extractable amounts are generally low (Si_o<0.1%, Al_o<0.2% and Fe_o<0.5%) and remain rather constant with depth. Only Fe and Mn extracted by DCB show a strong increase at and below the abrupt textural change, due to the higher content of the Fe–Mn oxides as compared to the bleached horizon.

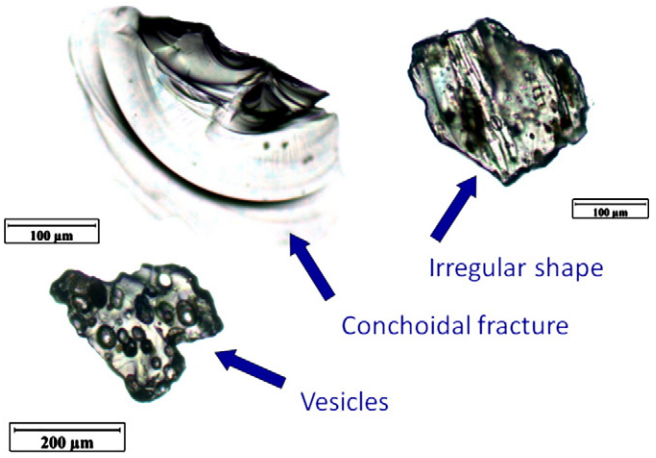

Fig. 11. Volcanic glass fragments in the sand fraction of the bleached horizon showing irregular shapes, conchoidal fractures and many vesicles due to incorporation of gas bubbles.

3.2. Hypothesis to explain the formation of the Vertic Planosols

Phytoliths are dominant in the bleached upper layer (Table 4; Fig. 10) and only in the silty infillings in the vertic horizon. Microscopic analysis of the sand fraction indicated that the bleached horizon contained many amorphous, colorless to light brown glass fragments (Fig. 11). Their irregular shapes, conchoidal fractures and the many vesicles (voids attributed to the incorporation of gas bubbles) are typical for volcanic glass. Based on these observations, another hypothesis than ferrolysis has been forwarded to explain the formation of these Vertic Planosols (Fig. 12). First the Vertisols were formed, with inside the vertic material formation of disorthic nodules due to hydromorphic conditions and the result of churning (Fig. 12a). Then, selective lateral erosion (removal of fines) resulted in an accumulation of many nodules at the surface; formation of a lag deposit (Fig. 12a'). Afterwards the Vertisols have been covered by in situ and/or transported volcanic ash (Fig. 12b); the latter by pedimentation upon erosion of the surrounding sloping areas. Volcanic ash deposits are very common in the surrounding areas. After the initial deposition, easily soluble elements, resulting from the weathering of volcanic glass (VG), were leached out or transformed into less soluble mineral components (Fig. 12c). Part of the dissolved

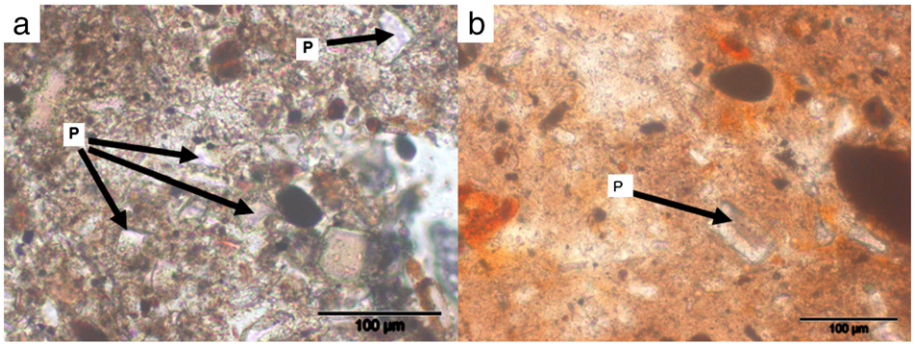

Fig. 10. Groundmass in plane polarized light of (a) the silty and bleached upper layer containing many phytoliths (P), and (b) the clayey soil material (vertic horizon) underneath having only few phytoliths.

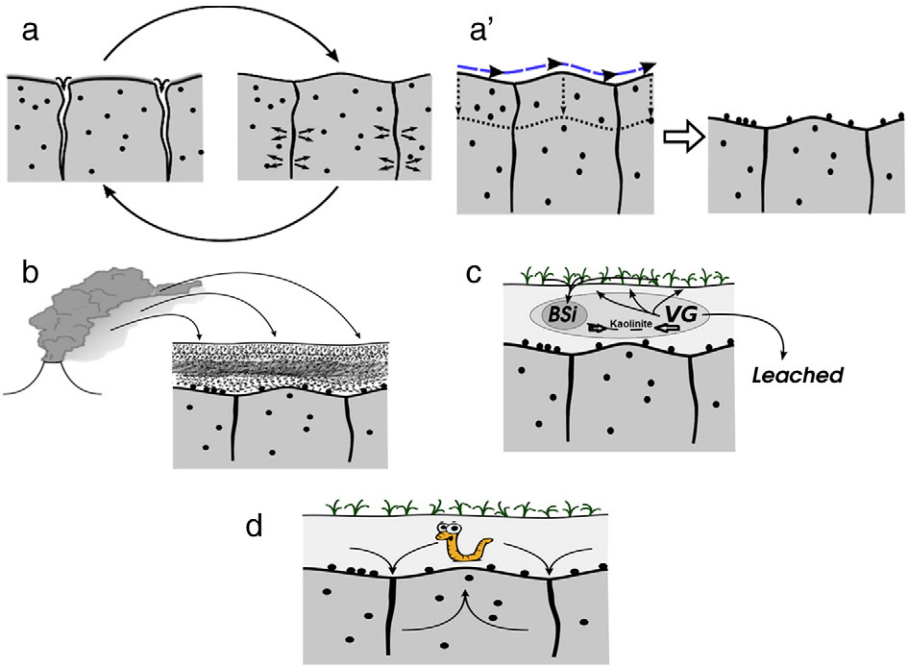

Fig. 12. Schematic representation of the proposed different steps in the formation of the Vertic Planosols in the Gilgel Gibe catchment: (a) churning in Vertisol results in formation of disorthic, rounded iron nodules; (a') removal of fines by selective lateral erosion results in formation of lag deposit of iron nodules; (b) Vertisol covered by in situ and/or reworked volcanic ash; (c) weathering of the volcanic glass (VG) releases Si, partly recycled by plants as phytoliths (BSi) or phytoliths, partly incorporated in secondary phases and partly leached out; and (d) mixing of soil material by biological activity, infilling of cracks and churning.

silica (H_4SiO_4) can be (i) taken up by grasses and polymerized in their tissue as phytoliths, (ii) incorporated in less soluble crystalline phases, or (iii) leached out. Thus, plants can exert a strong imprint on the Si continental cycle through the uptake and restitution of Si (Cornelis et al., 2010; Derry et al., 2005; Lucas, 2001). Indeed, phytoliths, ultimately cycled back to the soil as readily soluble biogenic silica (BSi: $SiO_2 \cdot nH_2O$), after decomposition of the organic matter (Fig. 12c). Mixing of the soil material by biological activity, infilling of cracks, and churning resulted in some geochemical blending of bleached and vertic materials (Fig. 12d). These geochemical blending and Si biocycling by grasses can explain the high phytolith content in the bleached horizon and in the silty infillings in the vertic horizon.

4. Conclusions

From the results of this analysis, it seems highly unlikely that ferrolysis can be called in to explain the genesis of Planosols in the Ethiopian highlands. Counter-indicative to ferrolysis at the point of abrupt textural change are the relatively high pH, presence of a sizeable reserve of weatherable minerals, feldspars and volcanic glass. The thin sections disclose high concentrations of phytoliths which are indicative of a high level of present and past biological recycling in the horizon above the textural change and in the vertic material. An alternative geogene hypothesis is put forward to explain the formation of these duplex soils. The studied profile should be considered as a soil complex with a A-(Bw)C-2Bw horizonation (2Bw being the vertic material), typical for volcanic areas. As Ethiopia is one of the mainstays of Planosols, it is suggested that WRB rethinks its strategy on soils with stagnic properties as there is room for rationalization. The selection of diagnostic characteristics takes into account their relationship with soil-forming processes. It is recognized that an understanding of these processes contributes to a better characterization of soils, but that they should not, as such, be used as differentiating criteria. This study shows that a major soil-forming process, unique for the Planosols, cannot explain the frequent association of Planosols with Vertisols in Ethiopia. This brings the Planosols surprisingly close to the Stagnosols. Other Reference Groups (e.g. Solonetz and Albeluvisols) maintain their position on account of a specific pedogenetic process leading to their existence. If the fundamental questions raised on the hypothesis of ferrolysis under the circumstances of the Ethiopian soilscape also apply to Planosol situations elsewhere in the world, one could argue to subdue either the Planosols or the Stagnosols to a lower level in the WRB system.

Acknowledgements

This study was partly funded by the 'Soil Fertility Project' within the Institutional Co-operation Programme between the Flemish Interuniversity Council (VLIR) and the Jimma University in Ethiopia.

References

Baldwin, M., Kellogg, C.E., Thorp, J., 1938. Soil classification. Soils and Men, Yearbook of Agriculture. USDA, Washington, USA.
Banks, E., Kosiner, E., Wertheim, G.K., 1966. Mössbauer effect in $FeMnO_3$. Journal of Chemical Physics 45, 1189–1191.
Barbiero, L., Mohan Kumar, M.S., Violette, A., Oliva, P., Braun, J.J., Kumar, C., Furian, S., Babic, M., Riotte, J., Valles, V., 2010. Ferrolysis induced soil transformation by natural drainage in Vertisols of sub-humid South India. Geoderma 156, 173–188.
Benyarku, C.A., Stoops, G., 2005. Guidelines for Preparation of Rock and Soil Thin Sections and Polished Sections. Quaderns DMACS 33, Universitat de Lleida, Spain. 84 pp.
Boivin, P., Favre, F., Hammecker, C., Maeght, J.L., Delarivière, J., Poussin, J.C., Wopereis, M.C.S., 2002. Processes driving soil solution chemistry in a flooded rice-cropped vertisol: analysis of long-time monitoring data. Geoderma 110, 87–107.
Boivin, P., Saejiew, A., Grunberger, O., Arunin, S., 2004. Formation of soils with contrasting textures by translocation of clays rather than ferrolysis in flooded rice fields in Northeast Thailand. European Journal of Soil Science 55, 713–724.
Boixadera, J., Poch, R.M., García-González, M.T., Vizcayno, C., 2003. Hydromorphic and clay-related processes in soils from the Llanos de Moxos (northern Bolivia). Catena 54, 403–424.
Brinkman, R., 1970. Ferrolysis, a hydromorphic soil forming process. Geoderma 3, 199–206.
Brinkman, R., Jongmans, A.G., Miedema, R., Maaskant, P., 1973. Clay decomposition in seasonally wet, acid soils: micromorphological, chemical and mineralogical evidence from individual argillans. Geoderma 10, 159–270.
Chartres, C.J., 1987. The composition and formation of grainy void cutans in some soils with textural contrast in South-eastern Australia. Geoderma 39, 209–233.

Cornelis, J.-T., Ranger, J., Iserentant, A., Delvaux, B., 2010. Tree species impact the terrestrial cycle of silicon through various uptakes. Biogeochemistry 97, 231–245.
Dahlgren, R.A., 1994. Quantification of allophone and imogolite. In: Amonette, J.E., Zelazny, L.W. (Eds.), Quantitative Methods in Soil Mineralogy. Soil Sci. Soc. Am, Madison, WI, USA, pp. 430–451.
Derry, L.A., Kurtz, A.C., Ziegler, K., Chadwick, O.A., 2005. Biological control of terrestrial silica cycling and export fluxes to watersheds. Nature 433, 728–731.
Dijkerman, J.C., Miedema, R., 1988. An Ustult–Aquult–Tropept catena in Sierra Leone, West Africa: I. Characteristics, genesis and classification. Geoderma 42, 1–27.
Drees, L.R., Wilding, L.P., Smeck, N.E., Senkayi, A.L., 1989. Silica in soils: quartz and disorders silica polymorphs. In: Dixon, J.B., Weed, S.B. (Eds.), Minerals in Soil Environments. Soil Sci. Soc. Am, Madison, USA, pp. 914–974.
Driessen, P., Deckers, J., Spaargaren, O., Nachtergaele, F., 2001. Lecture notes on the major soils of the World. World Soil Resources Report 94. FAO, Rome.
Dudal, R., 1971. Planosols. Joint Meeting of Commissions V and VI of the ISSS "Pseudogleys and Gleys — Genesis and Use of Hydromorphic Soils". Stuttgart, Hohenheim. 6–13 September.
Eaqub, M., Blume, H.P., 1982. Genesis of a so-called ferrolysed soil of Bangladesh. Zeitschrift für Pflanzenernährung und Bodenkunde 145, 470–482.
FAO, 2006. Guidelines for soil description, 4th Edition. FAO, Rome.
FAO/ISRIC/ISSS, 1994. World Reference Base for Soil Resources. Draft compiled and edited by O.C. Spaargaren. FAO, Wageningen/Rome. pp. 161.
FAO/ISRIC/ISSS, 1998. World Reference Base for Soil Resources, FAO World Soil Resources Reports 84. FAO, Rome. pp. 88.
FAO-UNESCO, 1974. FAO-UNESCO Soil Map of the World. UNESCO, Paris. pp. 59.
FAO-UNESCO, 1990. FAO-UNESCO Soil Map of the World. World Soil Resources Report 60 (Reprinted). FAO, Rome. pp.119.
Favre, F., Tessier, D., Abdelmoula, M., Genin, J., Gates, W.P., Boivin, P., 2002. Iron reduction and changes in cation exchange capacity in intermittently waterlogged soil. European Journal of Soil Science 53, 175–184.
Feijtel, T.C., Jongmans, A.G., Van Breemen, N., Miedema, R., 1988. Genesis of two Planosols in the Massif Central, France. Geoderma 43, 249–269.
Hobson, W.A., Dahlgren, R.A., 1998. Soil forming processes in vernal pools of northern California, Chico area. In: Witham, C.W., Bauder, E.T., Belk, D., Ferren Jr., W.R., Ornduff, R. (Eds.), Ecology, Conservation, and Management of Vernal Pool Ecosystems. Proceedings from a 1996 Conference. California Native Plant Society, Sacramento, CA, pp. 24–37.
Ingamells, C.D., 1966. Absorptiometric methods in rapid silicate analysis. Analytical Chemistry 38, 1228–1234.
IUSS Working Group WRB, 2007. World reference base for soil resources 2006. World Soil Resources Reports 103. FAO, Rome. http://www.fao.org/ag/agl/agll/wrb/. Electronic update 2007.
Kovda, I., Mermut, A., 2010. Vertic features. In: Stoops, G., Marcelino, V., Mees, F. (Eds.), Interpretation of Micromorphological Features of Soils and Regoliths. Elsevier, Amsterdam, pp. 109–127.
Lucas, Y., 2001. The role of plants in controlling rates and products of weathering: importance of biological pumping. Annual Review of Earth and Planetary Sciences 29, 135–163.
Montagne, D., Cornu, S., Le Forestier, L., Hardy, M., Josière, O., Caner, L., Cousin, I., 2008. Impact of drainage on soil-forming mechanisms in a French albeluvisol: input of mineralogical data in mass-balance modelling. Geoderma 145, 426–438.
O'Geen, A.T., Hobson, W.A., Dahlgren, R.A., Kelley, D.B., 2008. Evaluation of soil properties and hydric soil indicators for vernal pool catenas in California. Soil Science Society of America Journal 72, 727–740.
Omang, S.V., 1969. A rapid fusion method for decomposition and comprehensive analysis of silicates by atomic absorption spectrophotometry. Analytica Chimica Acta 46, 225–230.
Schaefer, C.E.R., Ker, J.C., Gilkes, R.J., Campos, J.C., da Costa, L.M., Saadi, A., 2002. Pedogenesis on the uplands of the Diamantina Plateau, Minas Gerais, Brazil: a chemical and micropedological study. Geoderma 107, 243–269.
Singh, L.P., Parkash, B., Singhvi, A.K., 1998. Evolution of the Lower Gangetic Plain landforms and soils in West Bengal, India. Catena 33, 75–104.
Soil Survey Staff, 2010. Keys to Soil Taxonomy11th Edition. USDA, Natural Resources Conservation Service, Washington DC. pp.338.
Stoops, G., 2003. Guidelines for Analysis and Description of Soil and Regolith Thin Sections. Soil Sci. Soc. Am, Madison, Wisconsin, USA. pp. 184.
Tadesse, S., Milesi, J.P., Deschamps, Y., 2003. Geology and mineral potential of Ethiopia: a note on geology and mineral map of Ethiopia. Journal of African Earth Sciences 36, 273–313.
Van Ranst, E., De Coninck, F., 2002. Evaluation of ferrolysis in soil formation. European Journal of Soil Science 53, 513–519.
Van Ranst, E., Verloo, M., Demeyer, A., Pauwels, J.M., 1999. Manual for the soil chemistry and fertility laboratory — analytical methods for soils and plants, equipment, and management of consumables. NUGI 835, Ghent University, Gent, Belgium. pp. 243.
Vandenberghe, R.E., De Grave, E., Landuydt, C., Bowen, L.H., 1990. Some aspects concerning the characterization of iron oxides and hydroxides in soils and clays. Hyperfine Interactions 53, 175–196.
Vandenberghe, R.E., De Grave, E., de Bakker, P.M.A., 1994. On the methodology of the analysis of Mössbauer spectra. Hyperfine Interactions 83, 29–49.
Vandenberghe, R.E., Barrero, C.A., Da Costa, G.M., Van San, E., De Grave, E., 2000. Mössbauer characterization of iron oxides and (oxy) hydroxides: the present state of the art. Hyperfine Interactions 126, 247–259.
Whittig, L.D., Allardice, W.R., 1986. X-ray diffraction techniques, In: Klute, A. (Ed.), Methods of Soil Analysis. Part 1. Physical and Mineralogical Methods, Second Edition. Agronomy Monograph 9, ASA-SSSA, Madison, Wisconsin, pp. 331–362.